



# THE BAND STRUCTURE AND OPTICAL PROPERTIES OF CDTE COMPOUNDS WERE ESTIMATED USING DENSITY FUNCTIONAL THEORY (DFT-LDA) AND (DFT-GGA)

Azhaar Jalal Brakhas, Abdulhadi Mirdan Ghaleb

University of Kirkuk, College of Science, Physics Department

abdldhadig4@gmail.com

## Abstract

In this article, we investigate the band structure and optical properties of cadmium telluride (CdTe) using density functional theory (DFT) with the CASTEP code. Using the local density approximation (LDA) and the generalized gradient approximation (GGA), we have applied plane-wave pseudo potential method to study the band gap energies ( $E_g$ ), partial density of state (PDOS), total density of state (TDOS) and optical properties like absorption ( $\alpha$ ), reflection (R), refraction index (n), dielectric constant ( $\epsilon$ ), conductivity ( $\sigma$ ) and extinction coefficient (k) were measured, with band gap energy 1.329 eV(LDA) and 1.392eV(GGA) are in good agreement with other theoretical calculations as well as available experimental data.

**Keyword:** Castep code; DFT (LAD), DFT (GGA), band gap, optical properties

## 1. Introduction

Semiconductor material such as II-VI have a many applications like a photovoltaic and photoconductive devices [1, 2] the one of semiconductor compound is cadmium telluride CdTe the crystalline structure and electronic characteristics of CdTe are similar to those of classic inorganic semiconductors. As a result, its electrical characteristics are well-known. Chelikowsky and Cohen, in particular, calculated its band diagram many years ago [3, 4]. Using empirical pseudo potential calculations with parameters suited to experimental data. Structure (zinc blende) is constructed with the lattice parameter 6.476 Å, at room temperature, CdTe displays a direct band gap approximately 1.5 eV [5]. Is one of chalcogenides family is CdS, CdSe and CdTe. these semiconductor material have many important application, such as solar cells, diodes, transistors, density optical memories, light emitting diodes and laser diode [6]. The underestimating of the band gap in CdTe, as other II-VI compounds, is linked to the underestimation of the binding energy of semi core Cd 4d levels in LDA. As a



result, the Cd 4d and Te 5p levels have an inappropriately large hybridization, pushing the top valence band, which is primarily formed of Te 5p levels, higher [7]. Numerous theoretical techniques are still in use today, including the ab initio method, density function theory, molecular dynamics, etc. To examine the structural [8-10], electrical [11-13], thermodynamic [14, 15], and optical properties of cadmium-based chalcogenides [16-18]. There have recently been extensive computations [19] of the structural, electronic, and optical characteristics of these compounds utilizing the full-potential linearized augmented plane wave (FP-LAPW) approach coupled with the local density approximation (LDA) [20] of the ex-change correlation energy to determine electronic and optical properties, respectively. There have been few studies to our knowledge that have employed the full potential computation FP-LAPW to compute the electrical, structural, and optical properties of these chalcogenide-based compounds.

## 2. Method of Calculation

All measurements were carried out by employing density functional theory (DFT) by using the standard local density approximation (LDA)-CAPZ and generalized gradient approximation (GGA-PBESOL) approach through using non-conserving pseudo potential and the relativistic treatment by using Cambridge serial total energy program (CASTEP) code [21]. Koelling-Hammon [22]. The electrons  $4d^{10}5s^2$  for Cd,  $5s^25p^4$  for the atoms were taken as the valence ones. In this work using customized energy cut off (450.0 eV) current cell volume ( $272.39\text{\AA}^3$ ) and ( $281.58\text{\AA}^3$ ) for LDA and GGA respectively. In the Brillouin region, the grid parameters were  $6\times 6\times 6$  k-points spread equally and calculated the band gap and total density of state (TDOS), partial density of state (PDOS) and optical properties.

## 3. Result and Discussion

### 3.1 Band Structure

Figure.1 (a and b) shows the band structures calculated for CdTe. The direct type of transitions describes the CdTe band gap. The results for the CdTe system's electronic energy structure demonstrate that the band gap is near the high-symmetry point G of the Brillouin zone CdTe band gap ( $E_g$ ) are lower than experimentally established specifications (1.329 eV) at LDA approximation and (1.396 eV) at GGA approximation. The total density of states (TDOS), the partial

density of states (PDOS) and the structure of the band all reflect their electrical properties. The density of the case is TDOS (see Figure 2).  $A = (0, 1/2, 1/2)$ ,  $b = (1/2, 0, 1/2)$ , and  $c = (1/2, 1/2, 0)$  are the cubic grid constant, which is the unit cell vectors of zinc-type structures Blind. The four units of the CdTe formula for each unit cell are Cd at  $(0, 0, 0)$  and Te at  $(1/4, 1/4, 1/4)$ . Figure 2(a and b) shows the locations and expected density of states (DOS) for CdTe calculated using LDA and GGA. According to the results of the LDA calculations, VB is made up of four bands, the lowest of which is made up of Te-5s states that have been slightly hybridized by Cd-4d states. Cd-4d bands primarily contribute to the following higher energy band. It has Te-5s and -5p bands that are mildly hybridized [23]. It has two well-defined peaks: one at lower energy is highly sharp and intense, while the other peak at greater energy has a smaller magnitude. The following smaller peak, which originates from hybridized Cd-5s- and Te-5p states, is placed at a higher energy level. The VB at the top and the CB at the bottom are not hybridized. The former comes from the Te-5p-states, whereas the latter comes from the Te-5p-states. Figure 2 shows the results of band structure computations for CdTe along high-symmetry directions within the Brillion zone. The band structure and band gap of CdTe were computed using the localized density approximation (LDA) and generalized gradient approximation (GGA) function in the software CASTEP, as shown in the figures, providing a band gap of roughly 1.329 eV for the CdTe at LDA and (1.396 eV) at GGA approximation, although the experimental band gap is claimed to be 1.4 eV [24]. Because the LDA function constantly underestimates the band gap, this occurs.

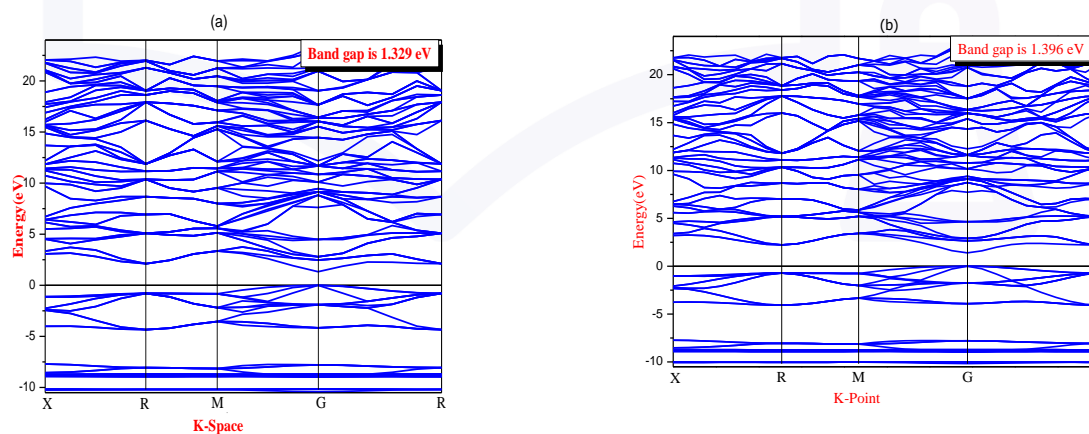


Fig. 1 shows the band gap structure of CdTe using the LDA and GGA approximations.

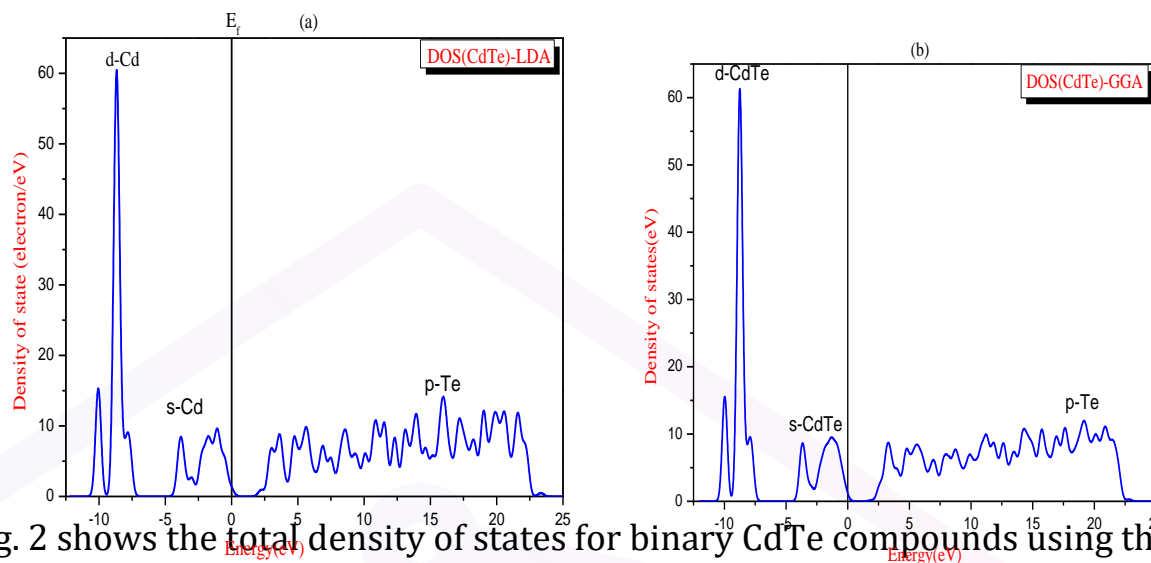


Fig. 2 shows the total density of states for binary CdTe compounds using the LDA and GGA approximations

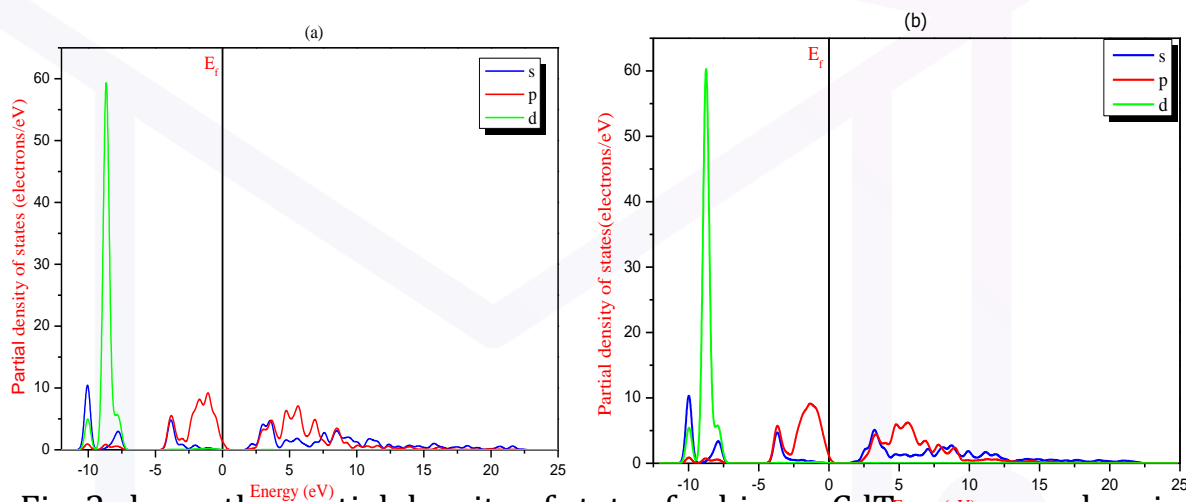


Fig. 3 shows the partial density of states for binary CdTe compounds using the LDA and GGA approaches.

### 3.2 Optical properties

Several publications have investigated the optical characteristics of CdTe in the reststrahlen region [25, 26]. According to the LDA and GGA approximations for CdTe, the following figures illustrate the energy band gap ( $E_g$ ) response functions ( $\epsilon_1$ ) and ( $\epsilon_2$ ), absorption coefficient ( $\alpha$ ), reflectivity ( $R$ ), refractive index ( $n$ ), conductivity ( $\sigma$ ), and extinction coefficient ( $k$ ). Their theoretical results were compared with the published experimental data [27]. The locations of all the peaks in the spectrum distribution of the optical spectra computed using DFT are pushed toward lower energy when compared to experimentally recorded ones. To correct the DFT underestimation of band gaps, a strict shift toward higher energies was used. All of the peak locations in the resulting optical spectra are



quite compatible with those determined experimentally. As a result, the underestimating of the band gap by DFT can be fixed using the k-independent scissors operator. Understanding a solid's electrical characteristics is aided by studying its optical characteristics, and optical conductivity of direct band gap It has been established that semiconductor binary compounds are optically active materials, and that these compounds' associated characteristics, such as their frequency-dependent dielectric function, The optical characteristics in this paper include An examination of the spectral distribution of optical spectra shows that the amplitude of the peaks corresponding to the fundamental absorption gap is overestimated in compared to experimental data. Additionally, for calculations of the imaginary part of the dielectric response function, only optical transitions from occupied to unoccupied states with a fixed  $E_p$   $k$  vector are taken into account. Furthermore, a lot of fine details are lost in the experimental resolution. It is discovered that the locations of the peaks in the computed and measured absorption and reflectivity spectra in this work and those in Ref. [27] disagree. The mismatch may be due to the different lattice characteristics between the CdTe thin films examined in this work and those examined in Ref. [27]. Exploring the optical characteristics of the CdTe is greatly wanted in order to determine its optoelectronic applications. Necessary optical qualities are needed for this. The main component of computed optical characteristics is the complex dielectric constant calculation, which measures the impact of an external electromagnetic field on a system's linear response. We utilize the mBJ functional to assess the optical characteristics because the estimated electronic band structure affects  $\epsilon(\omega)$ . In the definition of the complex dielectric function:  $\epsilon(\omega) = \epsilon_1(\omega) + i\epsilon_2(\omega)$ , the real and imaginary components of the function are denoted by  $\epsilon_1(\omega)$  and  $\epsilon_2(\omega)$ , respectively [28]. By knowing  $\epsilon(\omega)$ , one may calculate other important optical properties including the refractive index  $n(\omega)$ , the extinction coefficient  $k(\omega)$ , the optical reflectivity  $R(\omega)$ , the optical conductivity, and the absorption coefficient. This threshold is mostly caused by the transfer of electrons from the VB to the CB symmetry point for compound. Fig 8 (a,b) displays the real and imaginary portion of the dielectric function. The electronic component of the static dielectric constant, or zero frequency limit  $\epsilon_1(0)$ , is the most significant quantity in the spectra. It's computed values for CdTe-LDA and CdTe-GGA are 6.55 and 6.74, respectively. It is evident that the band gap and  $\epsilon_1(0)$  are inversely connected; a bigger energy gap results in a lower  $\epsilon_1(0)$  value.  $\epsilon_1(0)$  is higher for CdTe-GGA than for CdTe-LDA. The refractive index  $n(\omega)$  and extinction



coefficient  $k(\omega)$  of CdTe-LDA and CdTe-GGA are shown in Figs. 5 and 7, respectively. Up to 35 eV, the refractive index  $n(\omega)$  value spectrum spans a large energy range.  $n(\omega)$  and  $\epsilon_1(\omega)$  have comparable characters. The energy-dependent rise of  $n(\omega)$  to its highest values of 3.13 eV for CdTe-LDA and 3.39 eV for CdTe-GGA, respectively, is clearly shown in Figs. 5(a, b). This behavior of the peak in the transparency zone, which reaches minimum levels of 10.68 eV and 10.80 eV, respectively, illustrates the UV. The calculated values for CdTe-LDA and CdTe GGA's refractive index  $n(0)$  are 2.86 eV and 2.77 eV, respectively. This index similarly fluctuates inversely with the band gap. Additionally, it can be seen from Fig. 7(a, b) that local peaks in extinction coefficient  $k(\omega)$  correlate to the static section of  $\epsilon_1(0)$ . For compound  $n(\omega)$  and  $k(\omega)$  peak behavior is determined to be consistent overall, and it is well in line with previously published research on the topics. Our computed values of zero frequency reflectivity for CdTe-LDA and CdTe-GGA are 0.23 eV and 0.21 eV, respectively, based on Fig. 9(a,b). It should be noticed that while switching from CdTe-LDA to CdTe-GGA, the value of zero frequency reflectivity  $R(0)$  increases similarly to  $\epsilon_1(\omega)$ . It's interesting to note that where  $\epsilon_1(\omega)$  falls below zero, reflectivity achieves its highest value. When  $\epsilon_1(\omega)$  is negative, the materials are classified as metals. A compound's reflectivity is directly correlated with its metallicity, hence its  $R(\omega)$  value is maximum for a negative value of  $\epsilon_1(\omega)$ . The absorption coefficients  $\alpha(\omega)$  for the perovskites CdTe-LDA and CdTe-GGA are shown in Fig. 4(a,b). The tested materials' powerful absorption zones are justified. According to a comparison with Fig. 8(a,b), These distinct borders in the absorption coefficients are a feature of broad band gap semiconductor components which only permit photons with energy appropriate for stimulating an electron from the occupied levels of the valence band to the unoccupied levels in the conduction band to be detected into the material. Both of the perovskites' occurrence of high absorption areas between 13 and 15 eV may point to them as prospective candidates for use in UV frequency range optoelectronic devices. According to the measured optical conductivity (Fig. 6(a, b)), the optical conductivity of CdTe-LDA and CdTe-GGA respond to the applied energy at 1.36 eV and 1.30 eV, respectively.

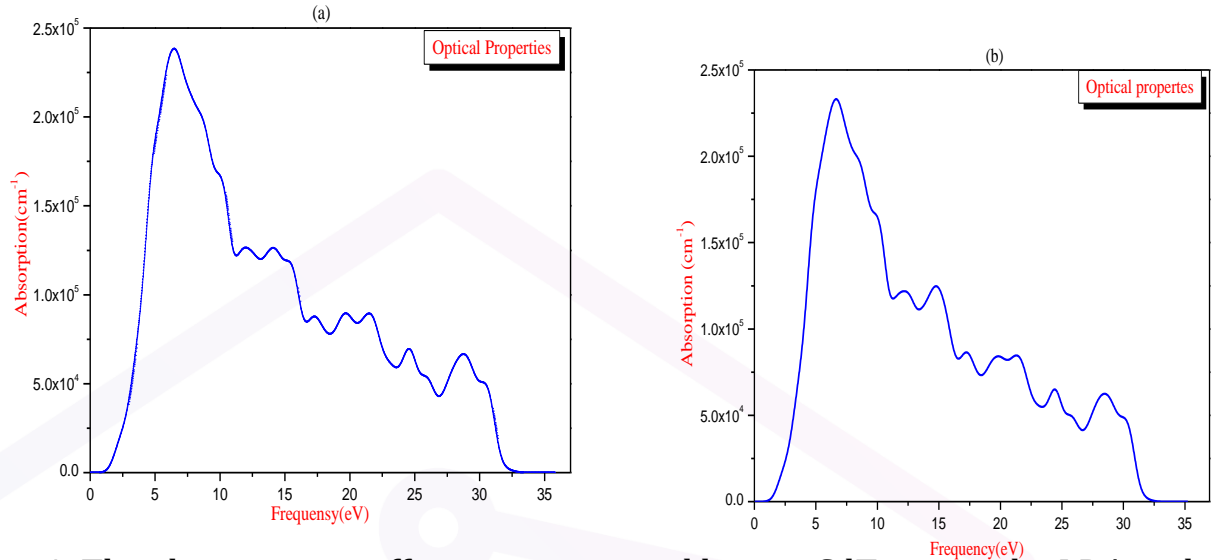


Fig. 4: The absorption coefficients compound binary CdTe using the LDA and GGA approaches.

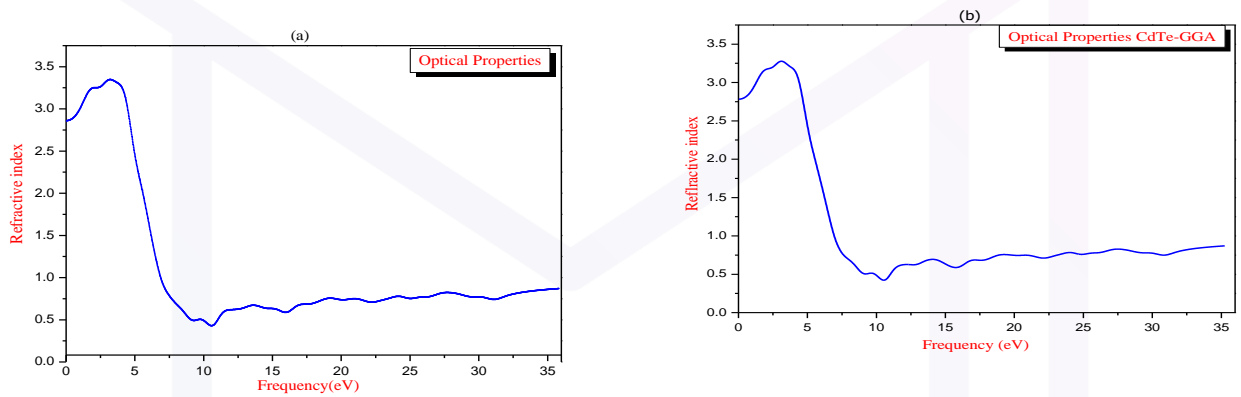


Fig. 5: The Refractive index compounds binary CdTe using the LDA and GGA approaches.

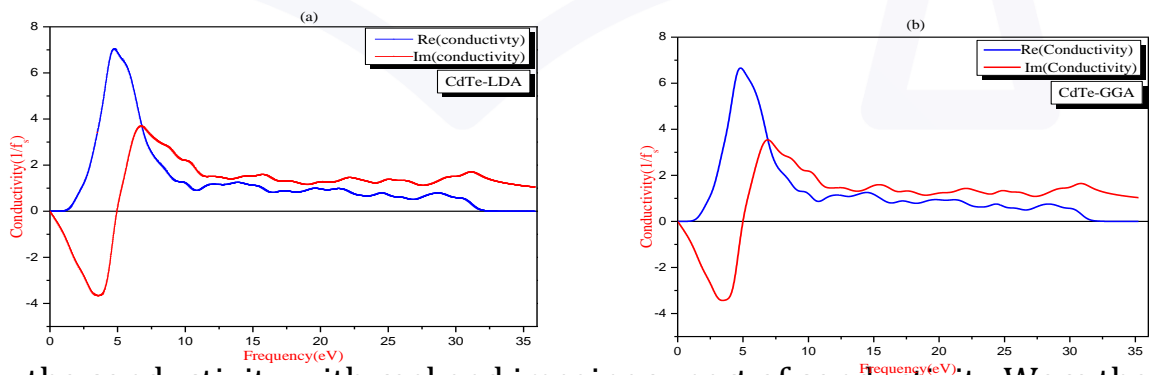


Fig.6: show the conductivity with real and imaginary part of conductivity. The real part is only positive value while the imaginary part is starting from negative part and going to positive part.

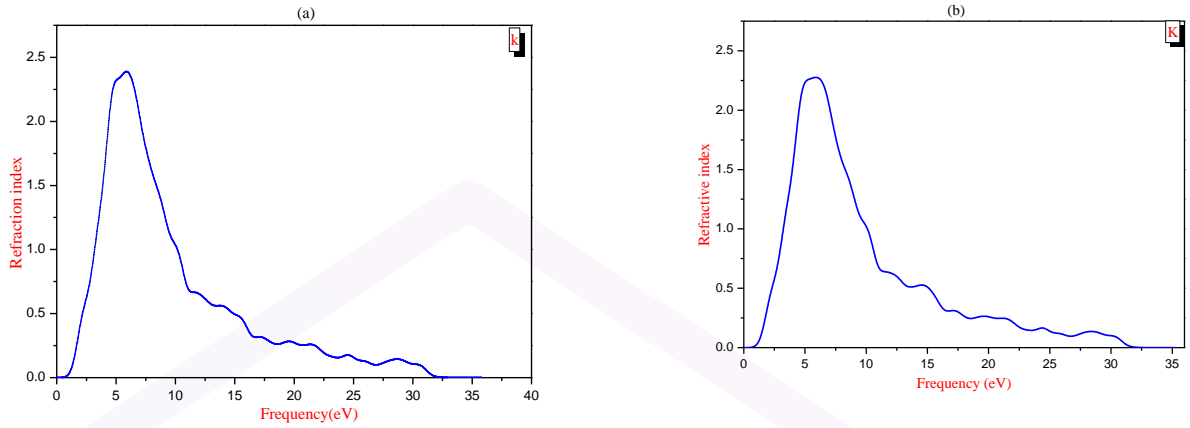


Fig.7: The refraction index compounds binary CdTe using the LDA and GGA approaches.

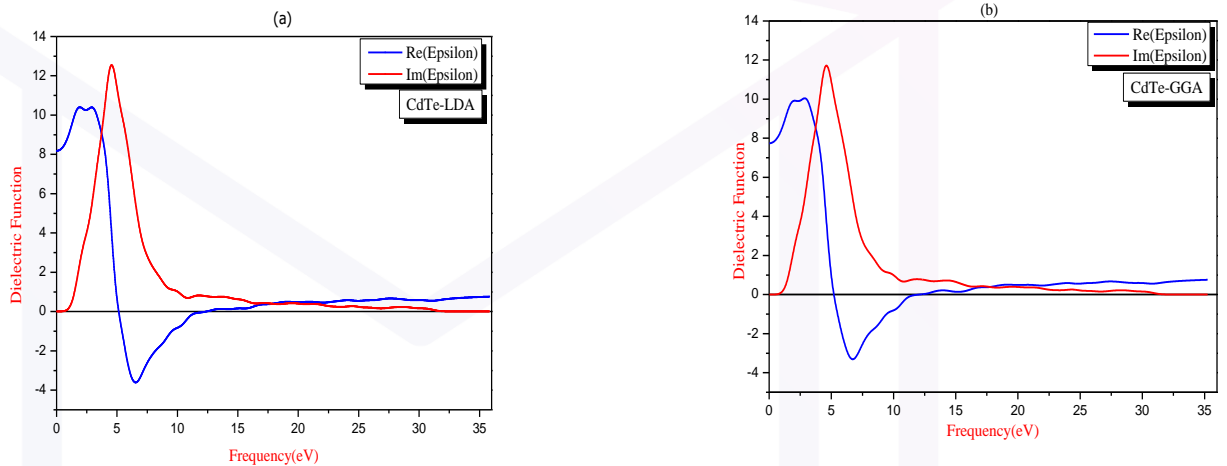


Fig 8: show the real and imaginary part of dielectric function where the peak of real part is 2.4 and the image is 10.8 for compounds binary CdTe using the LDA and GGA approaches.

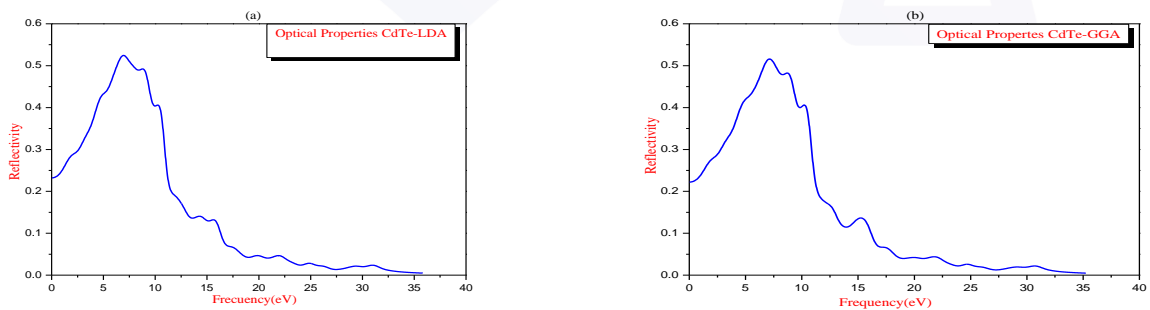


Fig. 9: The reflectivity compounds binary CdTe using the LDA and GGA approaches





## Conclusion

This paper investigates the band structure and optical characteristics of cadmium telluride (CdTe) using density functional theory (DFT) on the CASTEP code. To analyze the band gap energies ( $E_g$ ), total density of state (TDOS), and partial density of state (PDOS) and optical properties like absorption ( $\alpha$ ), reflection (R), refraction index (n), dielectric constant ( $\epsilon$ ), conductivity ( $\sigma$ ) and extinction coefficient (k) were measured. We employed the plane-wave pseudo potential approach using the local density approximation (LDA) and generalized gradient approximation (GGA).  $a = (0, 1/2, 1/2)$  a,  $b = (1/2, 0, 1/2)$  a, and  $c = (1/2, 1/2, 0)$  a are the unit-cell vectors of zinc-blende-type structures, where 'a' is the cubic lattice constant. Cd at (0, 0, 0) and Te at (1/4, 1/4, 1/4) are the four CdTe formula units per unit cell. With band gap energy (1.329 eV) and (1.396 eV) for LDA and GGA respectively, they are in good agreement with other theoretical calculations as well as available experimental data although the experimental band gap is claimed to be 1.4 eV.

## References

1. Capper, P. (Ed.). (1997). Narrow-gap II-VI Compounds for optoelectronic and Electromagnetic Applications (Vol. 3). Springer Science & Business Media.
2. Lovergine, N., Prete, P., Tapfer, L., Marzo, F., & Mancini, A. M. (2005). Hydrogen transport vapour growth and properties of thick CdTe epilayers for RT X-ray detector applications. *Crystal Research and Technology: Journal of Experimental and Industrial Crystallography*, 40(10-11), 1018-1022.
3. Chelikowsky, J. R., & Cohen, M. L. (1976). Nonlocal pseudopotential calculations for the electronic structure of eleven diamond and zinc-blende semiconductors. *Physical Review B*, 14(2), 556.
4. Paufler, P. (1986). Landolt-Börnstein. Numerical Data and Functional Relationships in Science and Technology. New Series. Editors in Chief: K.-H. Hellwege, O. Madelung. Group III: Crystal and Solid State Physics. Vol. 7: Crystal Structure Data of Organic Compounds. By W. Pies and A. Weiss. Part d: Key Elements: Si, Ge, Sn, Pb; B, Al, Ga, In, Tl; Be. dl: Key Elements Si, Ge, Sn, Pb. dl $\alpha$  Key Element Si. In cooperation with G. Will. Editors: K.-H. Hellwege AM Hellwege. Springer-Verlag, Berlin-Heidelberg-New York-Tokyo 1985 ....e
5. Venkatachalam, T., Velumani, S., Ganesan, S., & Sakthivel, K. (2008, April). Band structure and Optical properties CdTe and CdSn<sub>3</sub>Te<sub>4</sub> thin films. In AIP



- Conference Proceedings (Vol. 1004, No. 1, pp. 273-277). American Institute of Physics.
6. Sham, L. J., & Kohn, W. (1966). One-particle properties of an inhomogeneous interacting electron gas. *Physical Review*, 145(2), 561.
  7. Gürel, H. H., Akinci, Ö., & Ünlü, H. (2012). First principles calculations of Cd and Zn chalcogenides with modified Becke–Johnson density potential. *Superlattices and microstructures*, 51(5), 725-732.
  8. Wei, S. H., & Zhang, S. B. (2000). Structure stability and carrier localization in Cd X (X= S, Se, Te) semiconductors. *Physical review B*, 62(11), 6944.
  9. Benkhattou, N., Rached, D., Soudini, B., & Driz, M. (2004). High-pressure stability and structural properties of CdS and CdSe. *physica status solidi (b)*, 241(1), 101-107.
  10. Al-Douri, Y. (2003). The pressure effect of the bulk modulus seen by the charge density in CdX compounds. *Materials chemistry and physics*, 78(3), 625-629.
  11. Côté, M., Zakharov, O., Rubio, A., & Cohen, M. L. (1997). Ab initio calculations of the pressure-induced structural phase transitions for four II-VI compounds. *Physical Review B*, 55(19), 13025.
  12. Zakharov, O., Rubio, A., Blase, X., Cohen, M. L., & Louie, S. G. (1994). Quasiparticle band structures of six ii-vi compounds: ZnS, ZnSe, ZnTe, CdS, CdSe, and CdTe. *Physical Review B*, 50(15), 10780.
  13. Al-Douri, Y. (2003). Electronic and optical properties of  $Zn_xCd_{1-x}Se$ . *Materials Chemistry and Physics*, 82(1), 49-54.
  14. Tomasulo, A., & Ramakrishna, M. V. (1996). Quantum confinement effects in semiconductor clusters. II. *The Journal of chemical physics*, 105(9), 3612-3626.
  15. Kanoun, M. B., Sekkal, W., Aourag, H., & Merad, G. (2000). Molecular-dynamics study of the structural, elastic and thermodynamic properties of cadmium telluride. *Physics Letters A*, 272(1-2), 113-118.
  16. Merad, A. E., Kanoun, M. B., Merad, G., Cibert, J., & Aourag, H. (2005). Full-potential investigation of the electronic and optical properties of stressed CdTe and ZnTe. *Materials Chemistry and Physics*, 92(2-3), 333-339.
  17. Al-Douri, Y., Baaziz, H., Charifi, Z., Khenata, R., Hashim, U., & Al-Jassim, M. (2012). Further optical properties of CdX (X= S, Te) compounds under quantum dot diameter effect: Ab initio method. *Renewable Energy*, 45, 232-236.



18. Lahewil, A. S., Al-Douri, Y., Hashim, U., & Ahmed, N. M. (2012). Structural and optical investigations of cadmium sulfide nanostructures for optoelectronic applications. *Solar Energy*, 86(11), 3234-3240.
19. Deligoz, E., Colakoglu, K., & Ciftci, Y. (2006). Elastic, electronic, and lattice dynamical properties of CdS, CdSe, and CdTe. *Physica B: Condensed Matter*, 373(1), 124-130.
20. Perdew, J. P., & Wang, Y. (2018). Erratum: Accurate and simple analytic representation of the electron-gas correlation energy [Phys. Rev. B 45, 13244 (1992)]. *Physical Review B*, 98(7), 079904.
21. Schrödinger, E. (1995). *The interpretation of quantum mechanics: Dublin seminars (1949-1955) and other unpublished essays*. Ox Bow Press.
22. Segall, M. D., Lindan, P. J., Probert, M. A., Pickard, C. J., Hasnip, P. J., Clark, S. J., & Payne, M. C. (2002). First-principles simulation: ideas, illustrations and the CASTEP code. *Journal of physics: condensed matter*, 14(11), 2717.
23. Persson, C., & Zunger, A. (2003). s- d coupling in zinc-blende semiconductors. *Physical Review B*, 68(7), 073205.
24. Venkatachalam, T., Velumani, S., Ganesan, S., & Sakthivel, K. (2008, April). Band structure and Optical properties CdTe and CdSn<sub>3</sub>Te<sub>4</sub> thin films. In AIP Conference Proceedings (Vol. 1004, No. 1, pp. 273-277). American Institute of Physics.
25. Adachi, S. (1999). Zinc Telluride (ZnTe). In *Optical Constants of Crystalline and Amorphous Semiconductors* (pp. 473-486). Springer, Boston, MA.
26. Perkowitz, S. (1983). *Submillimeter solid-state physics. Infrared and millimeter waves*, 8, 71-125.
27. Adachi, S. (2013). *Optical constants of crystalline and amorphous semiconductors: numerical data and graphical information*. Springer Science & Business Media.
28. Fu, H., Wang, L. W., & Zunger, A. (1998). Response to "Comment on 'Comparison of the k·p and the direct diagonalization approaches for describing the electronic structure of quantum dots'" [Appl. Phys. Lett. 73, 1155 (1998)]. *Applied Physics Letters*, 73(8), 1157-1158.